

Induction of Purkinje fiber differentiation by coronary arterialization

Jeanette Hyer*[†], Mikkel Johansen*[‡], Aparna Prasad*, Andy Wessels[‡], Margaret L. Kirby[§], Robert G. Gourdie*[¶], and Takashi Mikawa*[¶]

*Department of Cell Biology, Cornell University Medical College, 1300 York Avenue, New York, NY 10021; [‡]Department of Cell Biology and Anatomy, Medical University of South Carolina, 171 Ashley Avenue, Charleston, SC 29425-2204; and [§]Institute of Molecular Medicine and Genetics, Medical College of Georgia, 1120 15th Street, Augusta, GA 30912-2640

Communicated by Setsuro Ebashi, National Institute for Physiological Sciences, Okazaki, Japan, September 7, 1999 (received for review June 7, 1999)

A synchronized heart beat is controlled by pacemaking impulses conducted through Purkinje fibers. In chicks, these impulse-conducting cells are recruited during embryogenesis from myocytes in direct association with developing coronary arteries. In culture, the vascular cytokine endothelin converts embryonic myocytes to Purkinje cells, implying that selection of conduction phenotype may be mediated by an instructive cue from arteries. To investigate this hypothesis, coronary arterial development in the chicken embryo was either inhibited by neural crest ablation or activated by ectopic expression of fibroblast growth factor (FGF). Ablation of cardiac neural crest resulted in $\approx 70\%$ reductions ($P < 0.01$) in the density of intramural coronary arteries and associated Purkinje fibers. Activation of coronary arterial branching was induced by retrovirus-mediated overexpression of FGF. At sites of FGF-induced hypervascularization, ectopic Purkinje fibers differentiated adjacent to newly induced coronary arteries. Our data indicate the necessity and sufficiency of developing arterial bed for converting a juxtaposed myocyte into a Purkinje fiber cell and provide evidence for an inductive function for arteriogenesis in heart development distinct from its role in establishing coronary blood circulation.

heart development | cardiac conduction system | coronary artery | retrovirus | neural crest

The contractive rhythm of the vertebrate heart depends on specialized tissue components involved in the generation and conductive spread of electrical excitation (1–3). The dominant pacemaking site in the heart is the sinoatrial node. From this focus of automaticity, activation is spread from cell to cell through atrial myocardium, eventually focusing into the atrioventricular node, where impulse propagation is delayed briefly before ventricular activation. After exit from the node, the propagating action potential accelerates along the atrioventricular bundle and its branched limbs, finally spreading into working ventricular muscle via a peripheral network of Purkinje fibers. Current understanding of the mechanisms regulating development of the cardiac pacemaking and conduction system is rudimentary (4–7). Fundamental issues, including whether common or different processes govern development of its disparate elements, remain unsettled. Our work in avian hearts has provided some progress on these questions, particularly in relation to the origin and differentiation of Purkinje fibers constituting the peripheral conduction system (4, 6, 8). By using replication-defective retroviruses, it was demonstrated that periarterial Purkinje fibers share common cellular progenitors with working myocytes (8). Of particular significance, this recruitment occurred in a site-specific pattern, with only those embryonic myocytes in direct proximity to coronary arterial vessels undergoing further differentiation into Purkinje fibers. Furthermore, we have recently shown (9) that embryonic myocytes in culture can be induced to convert to a Purkinje cell phenotype by endothelin—i.e., ET-1, a vascular cytokine secreted from arteries (10) in a shear stress-dependent manner (11). This latter observation led us to hypothesize a role for coronary arteries in

the process by which embryonic cardiomyocytes are induced to undergo further differentiation into Purkinje fibers.

Here, two complementary strategies are used to probe the relationship between arteriogenesis and the differentiation of Purkinje fibers in the embryonic chicken ventricle. In the first set of experiments we ask whether differentiation of the peripheral conduction network is suppressed by inhibition of the coronary arterial tree development. Ablation of the cardiac neural crest (NC) before its emigration from the dorsal neural tube results in systemic rearrangements of coronary vessel distribution in chicken embryos (12). If an inductive relationship exists between cardiac vascular and conductive tissues, then it is anticipated that the positioning of periarterial Purkinje fibers will change in concert with any changes to the ramification of coronary arteries in NC-ablated embryos. The second set of experiments involves examination of the effects of localized increases in the branching and density of coronary arteries provoked by retrovirus-mediated expression of fibroblast growth factor (FGF). Regionalized application or up-regulation of FGF has been shown to cause *de novo* induction of ectopic blood vessels at spatially discrete loci in a number of developmental models, including chick chorioallantoic membrane (13) and embryonic chicken heart (14). The results of the present study demonstrate that the coronary arterial bed has a decisive influence on the induction and patterning of the peripheral conduction system in the embryonic ventricle.

Materials and Methods

Laser Ablation of NC. Laser ablation of the cardiac NC was carried out on Hamburger and Hamilton stage 10 chicken embryos (*Gallus domesticus*) as has been described by Kirby *et al.* (15). Briefly, after a small window had been made in the egg shell and shell membrane, a small cut was made with a tungsten needle in the chorion and amniotic membrane to expose the cranial portion of the embryo. Subsequently, the intrinsic neural folds were bilaterally ablated in the regions of somites 1 to 3 by microprocessor-controlled pulsed illumination from a surgical laser focused through a Zeiss dissection microscope. The eggs were then resealed with Parafilm, placed in a humidified egg incubator at 37.5°C, and allowed to develop to the 15th day of embryonic incubation (E15). Control embryos were prepared and/or incubated in parallel with NC-ablated chicken embryos. At E15, the hearts were dissected from the embryos, fixed in 70% ethanol, and photographed by using a Zeiss dissection microscope. The samples were subsequently processed for paraffin

Abbreviations: NC, neural crest; FGF, fibroblast growth factor; En, embryonic day *n*; β -gal, β -galactosidase; anti-SMA, anti-smooth muscle actin; Cx42, connexin 42.

[†]J.H. and M.J. contributed equally to this work.

[¶]To whom reprint requests should be addressed. E-mail: gourdie@muscc.edu.

[¶]To whom reprint requests should be addressed. E-mail: tmikaw@mail.med.cornell.edu.

The publication costs of this article were defrayed in part by page charge payment. This article must therefore be hereby marked "advertisement" in accordance with 18 U.S.C. §1734 solely to indicate this fact.

embedding in frontal orientation, sectioned at 10 μm and slide mounted as has been detailed in earlier publications (8, 9, 16).

Retroviral Vectors and *in Ovo* Infection. The retrovirus used for genetic cell tagging is a replication-defective variant of a spleen necrosis virus co-encoding FGF and β -galactosidase (β -gal) (14, 17). Preparation of the viral vector, its propagation *in vitro*, and proof of helper virus-free stocks have been presented elsewhere (17). Viral concentrations of greater than 10^7 active virions per ml were obtained by ultracentrifugation of culture supernatant from packaging cells as has been described previously (18). After a small window had been opened in the shell and shell membrane of fertilized chicken eggs, a small cut was made with a tungsten needle in the chorion and amniotic membranes to expose the proepicardial organ. Viral suspensions of 5 nl, containing 100 $\mu\text{g}/\text{ml}$ Polybrene, were pressure injected *in ovo* into the proepicardial organ of Hamburger and Hamilton stage 17–18 embryos, as described (16). A parallel series of embryos injected with virus encoding only β -gal served as a control. The eggs were resealed with Parafilm and placed in a humidified incubator at 37.5°C to allow injected embryos to develop.

Histochemistry and Immunohistochemistry. The virus-infected embryos at E14–E18 were killed by cervical transection. Hearts were removed and fixed by immersion overnight in 2% paraformaldehyde (4°C in PBS) and processed for 5-bromo-4-chloro-3-indolyl β -D-galactoside (X-Gal) histochemistry in whole mounts as described previously (18). For immunohistochemistry and confocal microscopy, hearts were dissected from E14–18 chicken embryos. Single immunoperoxidase and single or double immunofluorescent labeling of histological sections with anti-smooth muscle actin (anti-SMA; Sigma), ALD58/sMHC (Developmental Studies Hybridoma Bank, Iowa City, IA), and anti- β -gal (5 Prime \rightarrow 3 Prime) antibodies were done according to methods detailed previously (8, 9, 19, 20). EAP3 mouse monoclonal antibodies against EAP300, a marker of chicken Purkinje fibers (8), were kindly provided by Gregory Cole (Ohio State Univ., Columbus, OH). The rabbit polyclonal antibody used (V15KR), with specificity for connexin 42 (Cx42)-containing gap junctions, has been previously characterized (9). This probe was custom produced in rabbits by Research Genetics (Huntsville, AL) against a synthetic peptide containing residues matching amino acids 256–270 of rat Cx40 and 271–280 of chicken Cx42. Immunofluorescent labelings using EAP3 (diluted 1:1000 in PBS) and V15KR (diluted 1:500 in PBS) were undertaken with protocols we have described in earlier publications (8, 9).

Quantitative Microstereology. The fractional volumes of coronary arteries and associated Purkinje fibers in NC-ablated and control hearts were estimated on immunolabeled histological sections by using a well-established point counting protocol (21). Microstereology was performed on three NC-ablated and four control hearts, each heart sectioned in frontal orientation (three sections were assessed per heart; at frontal, mid, and posterior planes). Intersections of coronary arterial profiles and adjacent Purkinje fiber cells with a M168 Weibel grid were counted at 40 independent microscope fields (40 \times objective) within each of the 21 histological sections assessed. Mean comparisons of volume fraction estimates between NC-ablated and control hearts were first made using Student's *t* test according to standard statistical practice. As the data showed slight deviation from normality, nonparametric Mann–Whitney tests were also done.

Results and Discussion

If an inductive relationship exists between vascular and conduction tissues in the heart, the positioning of intramural Purkinje fibers might be predicted to change in concert with changes in the ramification of coronary arteries. We tested this hypothesis

in vivo by probing for Purkinje fiber differentiation in the embryonic chicken heart after either inhibition or activation of coronary artery development. In the first set of experiments, coronary arterial branching was inhibited by ablating cardiac NC at E2 prior to its emigration from the dorsal neural tube (12, 15). NC-ablated embryos developed to E15, at which stage Purkinje fibers can be discriminated by expression of distinct marker genes (4). Arteries of non-operated and sham-operated controls (Fig. 1 *a* and *b*) and of NC-ablated hearts (Fig. 1 *e* and *f*) were identified by immunohistochemistry for vascular smooth muscle actin (19). The numbers and profiles of coronary arteries penetrating the ventricular myocardium were notably reduced in NC-ablated hearts. Those few histologically normal arteries that persisted after NC ablation were typically located within the basal ventricular myocardium. These alterations in the distribution of intramyocardial coronary arteries were not seen in control hearts (compare Fig. 1 *a* and *b* with *e* and *f*).

Differentiation of periarterial Purkinje fibers in NC-ablated embryos was then examined by probing for expression of EAP-300 (transitin) and Cx42, both early markers of conducting cells (4). In non-operated and sham-operated hearts, Purkinje fibers were distinguished from myocytes by elevated EAP-300 (Fig. 1*c*) and Cx42 (Fig. 1*d*). In NC-ablated embryos, EAP-300⁺ (Fig. 1*g*) and Cx42⁺ (Fig. 1*h*) cells were found only in areas adjacent to histologically normal arteries persisting within ventricular myocardium. There was no evidence of Cx42⁺/EAP-300⁺ Purkinje cells dispersed within ventricular myocardium independent of arteries. Hence, NC ablation did not result in a dissociation of intramural Purkinje fiber distribution from arterial branching patterns.

The volume densities (V_v) of the developing arterial bed and the periarterial Purkinje fiber network were quantified by microstereology in control and NC-ablated hearts (Table 1). Consistent with visual appraisal, this quantitative analysis indicated that there was a significant ($P < 0.01$) 66% reduction in the volume density (mm³ of artery per mm³ of myocardium) of intramyocardial coronary arteries in NC-ablated embryos compared with control embryos. The volume density of periarterial Purkinje fibers showed a comparably significant decrease ($P < 0.01$). These results, together with the immunolabeling data (Fig. 1), demonstrate that a reduction in Purkinje fiber differentiation resulting from NC ablation was accounted for by decreases in the density of coronary arterialization.

Although the above data suggest the necessity of coronary arteries for normal development of the Purkinje fiber network,

Table 1. Suppressed development of intramural coronary arteries and periarterial Purkinje fibers by NC ablation

Hearts	V _v , %	
	Intramural coronary arteries	Periarterial Purkinje fibers
NC-ablated	0.4 (0.06)	0.1 (0.02)
Control	1.2 (0.11)	0.3 (0.03)
Unpaired <i>t</i> test	$P < 0.01$	$P < 0.01$
Mann–Whitney	$P < 0.0001$	$P < 0.0001$

Quantitative microstereology reveals significant decreases in the volume density fractions (V_v, expressed as percentages) of cardiac tissue occupied by intramural coronary arterial profiles penetrating ventricular myocardium and periarterial Purkinje fibers in E15 hearts after NC ablation (15). The fractional volumes of coronary arteries and associated Purkinje fibers were scored on immunolabeled histological sections by using a well-established point counting protocol (21). Numbers in parentheses indicate the standard error. Comparisons of mean volume fraction estimates between NC-ablated and control hearts by Student's *t* test and nonparametric Mann–Whitney tests are presented as *P* values.

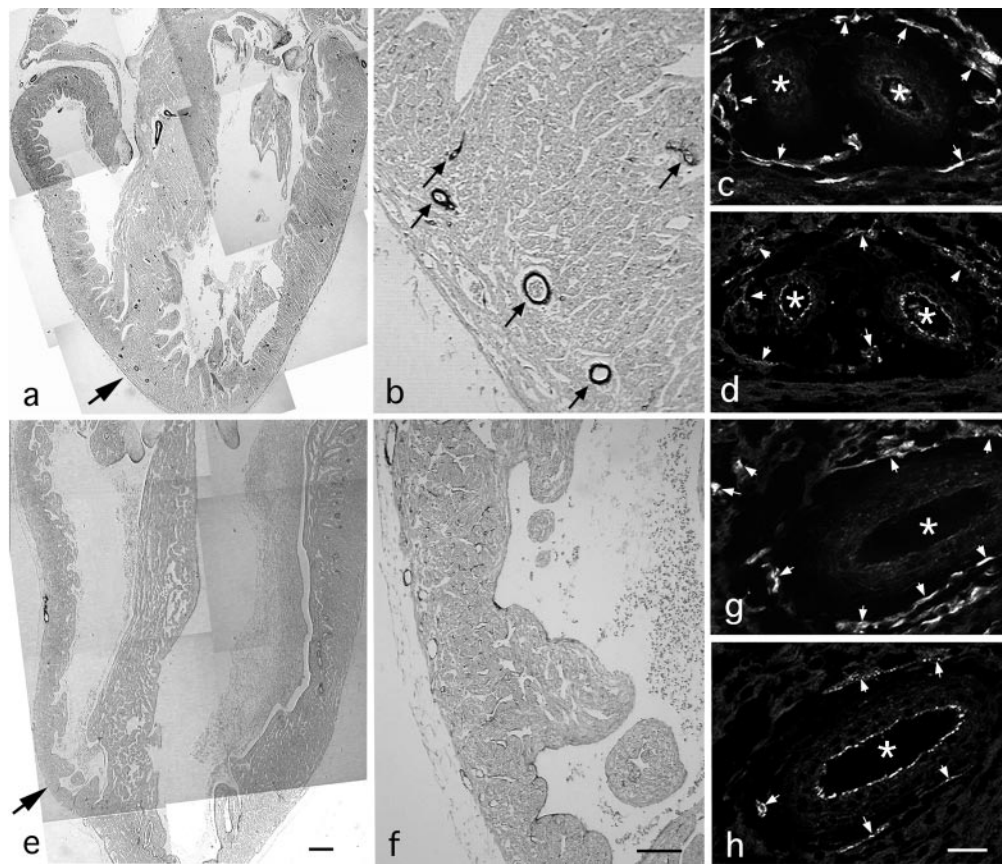


Fig. 1. Loss of Purkinje fibers following suppression of coronary arterial branching. Frontal sections of control (a–d) and NC-ablated (e–h) E15 hearts. Sections were immunolabeled with antibodies against smooth muscle actin (anti-SMA) (a, b, e, and f), EAP-300 (c and g), and Cx42 (d and h). Arrows on a and e indicate location of the higher magnification views shown in b and f, respectively. Arrows on b indicate anti-SMA-labeled intramural arteries. Arrows and asterisks on c, d, g, and h indicate Purkinje fibers and atrial lumen, respectively. No intramural arterial profiles are evident on f. (Scale bars a and e = 300 μm ; b and f = 100 μm ; and c, d, g, and h = 25 μm .)

it was unclear which step depends on the arterial system, the induction, survival, and/or terminal differentiation of Purkinje fibers. To address these questions, vessels were ectopically created in the embryonic heart. The potential for recruitment of myocytes to a Purkinje fiber phenotype was then examined at such sites of *de novo* vessel formation. Regionalized application or up-regulation of FGF has been shown to cause *de novo* induction of ectopic blood vessels at spatially discrete loci in a number of developmental models, including chick chorioallantoic membrane (13) and embryonic chicken heart (14). Coronary precursors were infected with a replication-defective retrovirus coencoding FGF and β -gal (14, 17) (Fig. 2a). A virus encoding only β -gal was used in control infections (8, 14) (Fig. 2a). The resulting treated and control hearts were examined at E18. Whole-mount X-Gal staining of these samples revealed that cells infected with either control β -gal virus (Fig. 2b) or FGF-producing virus (Fig. 2c and d) were distributed in the ventricle as discrete β -gal sectors. As demonstrated in our previous work, the cells constituting these sectors proliferate actively and migrate into the heart with other derivatives of the epicardial sheet (16, 18). Cells infected with control β -gal virus differentiated into normal epicardial and coronary vascular tissues (Fig. 2b) identical to uninfected stem cells. In contrast, and as we have shown previously (14), cells infected with FGF-virus developed vessel networks with abnormal branching patterns, and regions containing large numbers of FGF-virus-infected cells were often hypervascularized (Fig. 2c and d).

Ectopic Purkinje fiber differentiation was examined in these hearts by probing for the ALD58 antigen, a late marker of Purkinje fiber differentiation (8, 22, 23). In normal E18 and adult hearts, bona fide Purkinje fiber differentiation was detected in periarterial regions within the myocardium (Fig. 2e and f) and never occurred in the superficial myocardium underlying the epicardium (Fig. 2e). In control hearts infected with virus expressing only β -gal (red), no ALD58⁺ cells were identified in the superficial myocardium juxtaposed to β -gal⁺ epicardial cells (Fig. 2g). In contrast, ALD58⁺ Purkinje fibers (green) were found in myocardium adjacent to FGF-induced β -gal⁺ vessels (Fig. 2h and i). Importantly, the induction of ALD58⁺ cells was restricted to within one, or at most two, myocyte layers directly adjacent to ectopic vessels and never extended into deeper layers of muscle cells. The conversion of myocytes into ALD58⁺ Purkinje fibers was specifically dependent on the presence of arteries and was not the result of FGF. When the myocardium was directly infected with the same FGF-producing virus, ALD58⁺ Purkinje cells were never induced from infected or associated myocytes (negative data not shown). Moreover, in previous experiments *in vitro* we have shown that exogenous FGF is not able to elicit up-regulation of ALD58 in myocytes cultured from chicken embryos (9).

The above experimental approaches, resulting in either loss or ectopic differentiation of Purkinje fibers, demonstrate that the in-growth pattern of coronary arteries provides an inductive cue for differentiation and organization of the conduction system. The results are consistent with our previously pro-

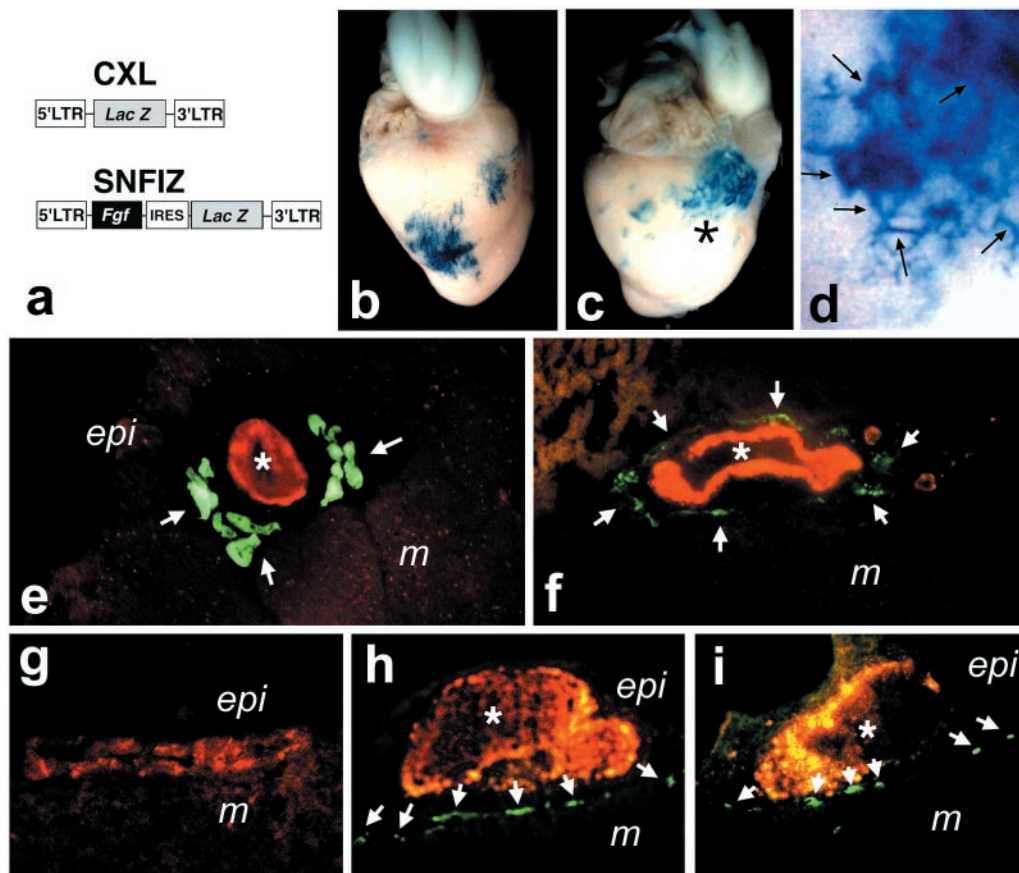


Fig. 2. Ectopic induction of Purkinje fibers at FGF-induced sites of hypervascularization. (a) Proviral structures of replication-defective retroviruses expressing only β -gal (8, 14) or coexpressing FGF4 and β -gal (14, 17) used for infection of coronary precursors *in vivo* on E3 (16, 18). (b and c) Hearts infected with control β -gal virus (b) or FGF-producing virus (c). (d) FGF-induced vessels (some prominent branches are arrowed) adjacent to the location indicated by the asterisk in c. (e–i) Cryosections double-labeled with ALD58 (green) and anti- β -gal (red) or anti-SMA (red) antibodies. Bona fide periarterial Purkinje fibers (green) in ventricular myocardium of an E18 (e) and adult (f) chicken. Arterial smooth muscle (red) is immunolabeled with anti-SMA in e and f. (g) No Purkinje fiber induction in the myocardium subjacent to epicardial cells (red) infected with control β -gal virus. (h and i) Induced ALD58⁺ (green) Purkinje fibers (arrows) in myocardium adjacent to β -gal⁺ (red) blood vessels induced by ectopic FGF secretion. Asterisks mark the lumen of the artificially formed vessels.

posed model (8). The inductive event appears to be a short-range paracrine interaction, since Purkinje fiber differentiation is restricted to a few myocyte layers juxtaposed to both bona fide and ectopic vessels. In chickens, coronary arteriogenesis begins with migration of vascular progenitors from the liver primordium into the heart on E3 (16, 18, 24), along with ingrowth of the epicardium. Endothelial progenitors organize into discontinuous channels (16, 25) and secondarily form early arterial vessels between E7 and E10 (26). Coronary arteries continue to anastomose and eventually establish a closed coronary vessel network around E14 (26). Importantly, differentiating Purkinje fibers become detectable between E10 and E15 (4), following initiation of the maturational phase of coronary arterial bed development and not before that time. Thus, Purkinje fiber differentiation may depend on a perfused and functional coronary arterial plexus. Physical proximity to organizing, but as yet functionally immature, vascular structures may not be sufficient to induce adjacent myocyte populations to differentiate into Purkinje fibers.

Consistent with this idea, embryonic myocytes convert *in vitro* to impulse-conducting Purkinje cells after exposure to a vascular paracrine factor endothelin (9) which is secreted in a shear-stress-dependent manner from coronary arteries (11). Its potential involvement *in vivo* is further supported by our observations of the expression pattern (K. Takebayashi-Suzuki and T.M., unpublished material) of endothelin-converting

enzyme, ECE (27, 28), a metalloprotease essential for converting an endothelin precursor into an active peptide. The *in situ* hybridization data in embryonic chicken heart revealed that ECE is induced in arterial beds only after they begin to function, but neither before that time nor in the venous system. The responsiveness of cultured embryonic myocytes to endothelin gradually declines as development proceeds (9). More mature cardiocytes, responding to endothelins, undergo hypertrophy (29), instead of conversion to Purkinje fiber cells. Thus, differentiation of Purkinje fibers may be spatiotemporally confined both by an inductive signal whose activity is localized to the arterial bed and by developmental changes in the response of myocytes to that signal.

Coronary arteries are vital for survival of both growing and mature cardiac muscle. In addition to having their well-established function in perfusion, our data demonstrate that coronary arteries in the embryonic heart play a central and previously unrecognized role in differentiation and organization of impulse-conducting Purkinje fibers. This newly uncovered inductive potential of arteriogenesis may provide for future therapeutic approaches to regeneration and/or repair of cardiac conduction systems damaged by disease or congenital abnormality. The future studies should address whether terminal differentiation of Purkinje fibers is a direct result of the arterial system. Finally, that in-growing vessels act only in the developing heart to foment three-dimensional pattern during development seems unlikely. Recent retroviral fate

mapping studies suggest a role for interactions between in-growing arteries and central nervous system cells in selection of glial cell fate and distribution of astrocytic pattern in the developing rodent brain (30). Interestingly, this induction of astrocytic differentiation is accompanied by up-regulation of specific intermediate filament genes, including nestin, a mammalian homolog of chicken EAP-300 (transitin), a neurofilament also expressed by cardiac Purkinje fibers (4). It is speculated that analogs of the inductive process we describe in the embryonic heart may well be involved in the generation of

complexity in other well-vascularized organ systems, including the developing brain.

The assistance of Mrs. Sandra Klatt and Aimee Phelps is acknowledged with gratitude. This work was supported by grants from the National Heart, Lung and Blood Institute (TM-HL62175, HL56987, HL54128, RGG-HL56728, AW-HL52813), the National Science Foundation (RGG-9734406), and the March of Dimes Birth Defects Foundation (RGG-FY95 1145, FY96 1139). R.G.G. is an Early Career Scholar of the National Science Foundation. T.M. is an Irma T. Hirsch Scholar.

1. Tawara, S. (1906) *Das Reizleitungssystem des Säugetierherzens* (Gustav Fischer, Jena, Germany).
2. Goldenberg, M. & Rothberger, C. J. (1936) *Pflügers Arch.* **237**, 295–306.
3. Bozler, E. (1943) *Am. J. Physiol.* **138**, 273–282.
4. Gourdie, R. G., Kubalak, S. & Mikawa, T. (1999) *Trends Cardiovasc. Med.* **9**, 18–26.
5. Schiaffino, S. (1997) *Circ. Res.* **80**, 749–750.
6. Mikawa, T. & Fischman, D. A. (1996) *Annu. Rev. Physiol.* **58**, 509–521.
7. Gorza, L., Vettore, S. & Vitadello, M. (1994) *Trends Cardiovasc. Med.* **4**, 153–159.
8. Gourdie, R. G., Mima, T., Thompson, R. P. & Mikawa, T. (1995) *Development (Cambridge, U.K.)* **121**, 1423–1431.
9. Gourdie, R. G., Wei, Y., Kim, D., Klatt, S. C. & Mikawa, T. (1998) *Proc. Natl. Acad. Sci. USA* **95**, 6815–6818.
10. Yanagisawa, M., Kurihara, H., Kimura, S., Tomobe, Y., Kobayashi, M., Mitsui, Y., Yazaki, Y., Goto, K. & Masaki, T. (1988) *Nature (London)* **332**, 411–415.
11. Yoshizumi, M., Kurihara, H., Sugiyama, T., Takaku, F., Yanagisawa, M., Masaki, T. & Yazaki, Y. (1989) *Biochem. Biophys. Res. Commun.* **161**, 859–864.
12. Hood, L. A. & Rosenquist, T. H. (1992) *Anat. Rec.* **234**, 291–300.
13. Wilting, J., Christ, B. & Bokeloh, M. (1991) *Anat. Embryol.* **183**, 259–271.
14. Mikawa, T., Hyer, J., Itoh, N. & Wei, Y. (1996) *Trends Cardiovasc. Med.* **6**, 79–86.
15. Kirby, M. L., Kumiski, D. H., Myers, T., Cerjan, C. & Mishima, N. (1993) *Dev. Dyn.* **198**, 296–311.
16. Mikawa, T. & Gourdie, R. G. (1996) *Dev. Biol.* **173**, 221–232.
17. Mima T., Ueno, H., Fischman, D. A., Williams, L. T. & Mikawa, T. (1995) *Proc. Natl. Acad. Sci. USA* **92**, 467–471.
18. Mikawa, T. & Fischman, D. A. (1992) *Proc. Natl. Acad. Sci. USA* **89**, 9504–9508.
19. Huang, G. Y., Wessels, A., Smith, B. R., Linask, K. K., Ewart, J. L. & Lo, C. W. (1998) *Dev. Biol.* **198**, 32–44.
20. Gang, C., Gourdie, R. G. & Thompson, R. P. (1999) *BioTechniques* **27**, 438–440.
21. Weibel, E. R. (1979) in *Stereological Methods* (Academic, London), Vol. I, pp. 301–311.
22. Sartore, S., Pierobon-Bormioli, S. & Schiaffino, S. (1988) *Nature (London)* **274**, 82–84.
23. Gonzalez-Sanchez, A. & Bader, D. (1985) *J. Cell Biol.* **100**, 270–275.
24. Poelmann, R. E., Gittenberger-de Groot, A. C., Mentink, M. M., Bokenkamp, R. & Hogers, B. (1993) *Circ. Res.* **73**, 559–568.
25. Waldo, K. L., Willner, W. & Kirby, M. L. (1990) *Am. J. Anat.* **188**, 109–120.
26. Rychter, Z. & Ostradal, R. (1971) *Folia Morphol.* **16**, 113–124.
27. Xu, D., Emoto, N., Giaid, A., Slaughter, C., Kaw, S., deWit, D. & Yanagisawa, M. (1994) *Cell* **78**, 473–485.
28. Yanagisawa, H., Yanagisawa, M., Kapur, R. P., Richardson, J. A., Williams, S. C., Clouthier, D. E., de Wit, D., Emoto, N. & Hammer, R. E. (1998) *Development (Cambridge, U.K.)* **125**, 82–836.
29. Ito, H., Hirata, Y., Hiroe, M., Tsujino, M., Adachi, S., Takamoto, T., Nitta, M., Taniguchi, K. & Marumo, F. (1991) *Circ. Res.* **69**, 209215.
30. Zerlin, M. & Goldman, J. E. (1997) *J. Comp. Neurol.* **387**, 537–543.